Chapter 3

Physics of Liquid Argon Time Projection Chamber

Chapter 3 Opening

3.1 Overview of LArTPC

The Liquid Argon Time Projection Chamber (LArTPC) is the technology of choice for Fermilab's neutrino program, due to its ability to facilitate a high rate of neutrino interactions while maintaining exceptional spatial, calorimetry, and timing resolution. Moreover, the abundant availability of argon is ideal for scaling detectors to a large target mass, reaching up to tens of kilotons of liquid argon. Notably, the Short-Baseline Neutrino (SBN) programme comprises of three LArTPC experiments of sizes in the hundreds of tons, located along the Booster Neutrino Beam (BNB): the Short-Baseline Near Detector (SBND), MicroBooNE, and ICARUS [1]. This novel technology will also be utilised at the upcoming long baseline Deep Underground Neutrino Experiment (DUNE), of which its far detector is composed of four LArTPCs, boasting a total volume of 70 kilotons [2].

A diagram illustrating the general operation principle of a LArTPC is provided in Fig. 3.1. Charged particles resulting from a neutrino interaction ionise argon atoms as they traverse through the detector medium, also producing scintillation photons in the process. A high negative voltage is applied at the cathode plane, creating an electric field under which the ionisation electrons drift towards the anode. Once arrive at the anode, the ionisation electrons induce signals on the inner wire planes and finally collected on the outermost plane. The combination signals from these planes result in a high granularity three dimensional image of the interaction. Since the wire planes are transparent to the scintillation photons, an additional Photon Detection System (PDS) is installed behind the wire planes, gaining precise timing information of the interaction.

Specifically chosen for the precise measurement of neutrino cross sections, liquid argon has a high density of 1.39 gcm^{-3}, and a high atomic mass of 40. The probability of neutrino interactions increases with the number of nucleons in the detector volume, and liquid argon, therefore, enables a high rate of neutrino interactions. Furthermore, given that argon is a noble element, the energy deposited by particles traversing through the medium can only be used for ionising electrons and producing scintillation photons. This maximises the efficiency of energy transfer into observable signals for detection. Additionally, liquid argon has a very high electron mobility, allowing for ionisation electrons to quickly drift under an electric field. Recent technology advancements in purifying argon has resulted in stable and ultra pure argon, which ensures that electrons can transverse the drift distance towards detection without being captured []. Consequently, liquid argon continues to stand out as an advantageous target material for neutrino experiments.

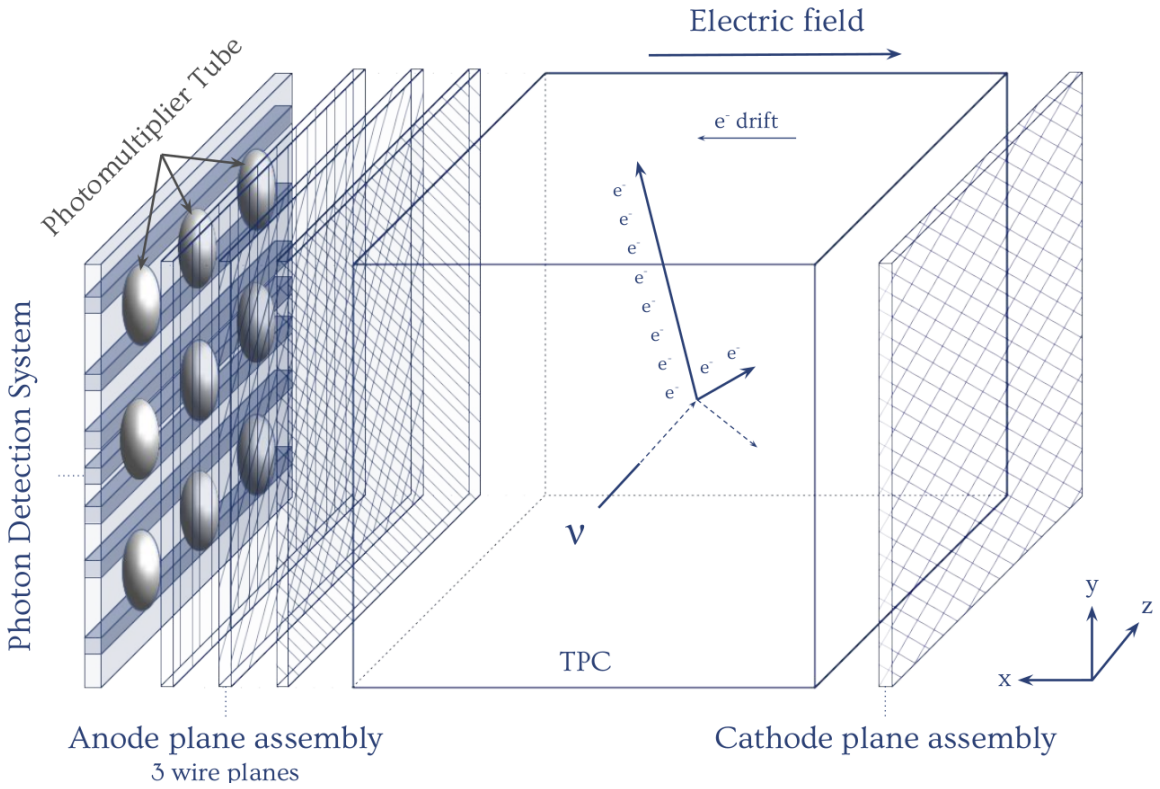

Fig. 3.1 Illustration of a general-purpose LArTPC. An example neutrino interaction is shown, which produces two charged tracks (solid lines) and a neutral track (dashed line). The charged tracks produce ionisation electrons, which drift under an electric field towards the anode. The neutral track does not ionise the argon atoms and thus not directly visible in the detector. [3].

The following sections will delve into the details of the principle operations of a LArPTC. In Sec. 3.2, a comprehensive discussion is presented on particle interactions with the liquid argon to produce ionisation electrons and scintillation photons. Following that, Sec. 3.3 outlines the propagation of the resultant electrons and photons through the liquid argon medium. Finally, Sec. 3.4 provides an insight into the detection mechanism of the ionisation electrons and scintillation photons using the wire planes and a complex PDS respectively.

3.2 Particle Interactions in Liquid Argon

3.2.1 Ionisation Electrons

Particles traversing a medium like liquid argon experience energy loss via ionisation, producing ionised electrons as secondary particles. The typical energy loss profile for particles is shown in Fig. **??**, specifically for a muon traversing in a copper medium but the principle is applicable to liquid argon. This plot shows the stopping power,the energy loss per unit length divided by the density of the target medium, against the momentum of the traversing particle. At the energy ranges relevant in LArTPC, heavy particles like muons, pions, and protons, lose energy as described by the Bethe-Block formalism. For lighter and highly relativistic particles, such as > 100 MeV electrons and photons in liquid argon, the energy loss mechanism is primarily via radiative effects. An example for both of these event topologies are shown in Fig. **??**.

Muons, pions and protons traverse liquid argon and interact electromagnetically with its atom, primarily via Multiple Coulomb Scattering (MCS) and freeing electrons along their trajectories. Since these trajectories are typically straightly lines, they are referred to as *tracks*. The MSC process is dependent on the particle momentum. The energy deposited per unit length via ionisation, dE/dx, is typically constant in the Minimum Ionising Particle (MIP) but arises when the particle comes to a stop, called Bragg peak. The energy loss profile is dependant on the particle mass, and thus often used to perform Particle IDentification (PID) [], most effective for protons separation from muons and pions. The energy depositions for tracks in the MIP region is described a Landau-Gaussian Convolution (LCG), where the Most Probable Value (MPV) describes the most deposited region.

Electrons with energy above the critical energy, the energy at at which losses by ionisation are equal to losses by radiation, deposit energy via radiative effects. This typically produce cones of electromagnetic activities, also known as *showers*. The critical energy for electron in liquid argon is 32.8 MeV. Photons are neutral particles and therefore can travel some distance without ionising and before depositing energy inside the liquid argon. This produces a gap between the interaction vertex and the start of the shower, called *conversion gap*. This distance is plotted in Fig. **??**. At low energies, photon lose energy primarily via Compton scattering but at higher energy, pair production is the dominating effects, producing an e^+e^- pair. Both the energy loss profiles and the conversion gaps can be used for distinguishing between electrons and photons.

3.2.2 Scintillation Photons

Moreover, charged particles traversing liquid argon also produce scintillation photons as secondary particles, through two different processes that both result in an argon excimer (Ar_2^*) shown in Fig. **??**. The first process is known as self-trapped exciton. This begins with the charged particle does not have sufficient energy for ionisation, and hence, excites the argon atom upon collision instead. The excited argon atom (Ar^*) self-traps with another argon atom, forming an argon excimer (Ar_2^*). The second process is known as recombination. Ionisation in liquid argon produce a free electron and an argon ion (Ar^+). The electron can either escape and drift towards the anode for detection, or recombine with an argon ion and an argon atom (Ar), forming an argon excimer (Ar_2^*).

The argon excimer is short-lived and undergoes radiative decay into two ground-state argon atoms, producing scintillation photons with wavelength of 128 nm in the Vacuum UltraViolet (VUV) range []. The timing constant of the decay depends on the excitation state. The singlet state has a shorter mean lifetime with a decay constant $\tau_1 \approx 6$ ns, while the triplet has a longer mean lifetime with a decay constant $\tau_3 \approx 1.5 - 1.6$ μs []. These are referred as the fast (or prompt) and slow (or late) components, respectively. The time-dependent probability of light emission in pure liquid argon can therefore be modelled as

$$l(t) = \frac{A_1}{\tau_s} \exp\left(-\frac{t}{\tau_1}\right) + \frac{A_3}{\tau_3} \exp\left(-\frac{t}{\tau_3}\right) \tag{3.1}$$

where A_1 and A_3 are the decay amplitudes of the singlet and triplet states respectively. For a MIP muon, the ratio of singlet-to-triplet state is $\approx 1:3$, where $A_1 \approx 0.25$ and $A_3 \approx 0.75$ [].

Liquid argon is an excellent medium to produce scintillation light, the scintillation light yield is approximately 40000 photons per MeV of deposited energy [] in the absence of an electric field. In a typical electric field at 500 V/cm, as in SBND, the light yield decreases to approximately 20000 photons per MeV of deposited energy at 500 V/cm [], due to free electrons are drifted before recombination can occur. Ionisation density created by interacting particles can affect local recombination factor, and thus the light yield. At high ionisation density, this can lead to quenching effect, further reducing the light yield /cite. Contaminants in the liquid argon such as oxygen and nitrogen also contributes to the quenching effect, by absorbing the energy without emitting any photons [].

3.2.3 Recombination

The electron-ion recombination, one of the two processes to produce scintillation photon, occurs immediately within 1-2 ns following the electron ionisation process. As shown in Fig. **??**, the resulting number of ionisation electrons and photons are anti-correlated, driven by the recombination R

$$R = W_{ion} \cdot \frac{dE/dx}{dQ/dx} \tag{3.2}$$

where $W_{ion} = 23.6$ eV is the energy required to ionise and argon and $\frac{dQ}{dx}$ and $\frac{dE}{dx}$ is the charge and energy loss per unit length respectively []. If not taken into account, the recombination can result in underestimating energy loss due to ionisation.

A popular model to describe this effect is the Box Model [], which the inverse Box Model equation is modelled as []

$$\frac{dE}{dx} = \frac{1}{\beta}\left[\exp\left(\beta W_{ion}\frac{dQ}{dx}\right) - \alpha\right] \tag{3.3}$$

where α and β are tunable parameters. Recombination is highly dependent on the electric field and the local charge density. The effects of the electric field intensity is folded into the β parameter. ArgoNeuT experiment has recently measured the recombination factor in LArTPC [], and demonstrated a data-driven study on recombination factor. The resulting “Modified Box Model" with parameter $\alpha = 0.93$ and $\beta = 0.30$ MeV/cm best describes the recombination effects in LArTPC.

The number of ionisation electrons and scintillation photons produced from interacting particles are highly dependent on the electric field, as discussed in Sec. **??**. The stronger the electron field, the higher number of ionisation electrons are separated from the argon ions and drifted towards the anode for detection before recombination can occur. Conversely scintillation photon is produced in the recombination process and the recombination factor is reduced in the presence of an electric field, decreasing the amount of light. This leads to an anti-correlation between the ionisation charge Q and the scintillation light L. Fig. **??** shows the Q and L yield as a function of the electric field strength for several noble gas elements. SBND detector has an electric field of 500 V/cm, which is the region where the energy deposition to ionisation electrons and scintillation electrons are approximately equal.

3.3 Transportation of Particles in Liquid Argon

3.3.1 Electrons Drift

Diffusion

Ionised electrons that do not recombine are drifted towards the anodes under the effects of electric field, by applying a high negative voltage to the cathode. Under the conditions of SBND with a drift field of 500 V/cm and a temperature of 87 K, the drift velocity of electrons is 0.16 cm/μs.

As the ionised electrons drift, they undergo diffusion, which perturbs the trajectory of the electrons due to various effects, such as inelastic collisions. Diffusion causes the shape of of a cloud of electrons produced in a point like energy deposition to grow in volume while drifting. The effects increase with respect to the drift distance and smear both spatial and temporal resolutions.

The Gaussian profile resulting from the response function of the charge deposition on the wire can therefore be modelled as

$$\sigma^2(t) = \sigma_0^2 + \left(\frac{2D}{v_d^2}\right) t \tag{3.4}$$

The observed profile σ depends on the initial profile (no diffusion) σ_0, the drift velocity v_d, the drift time t and the diffusion coefficient D []. Diffusion is parameterised in both longitudinal direction D_L (parallel to the drift ad field direction) and transverse direction D_T (perpendicular to the drift and field direction). Longitudinal diffusion is due to individual electron arriving on the wire earlier and later within the electron cloud moving at the drift velocity. Transverse diffusion broadens the cross section of the electron cloud arriving the anode plane, causing electrons migrating to neighbouring wires. Under the same conditions as the SBND detector, the diffusion coefficients have been measured to be $D_L = 7.2$ cm^2/s and $D_T = 12.0$ cm^2/s [].

Attenuation

Moreover, drifting electrons can be captured by electronegative impurities present in the argon medium, mostly commonly oxygen and water []. This results in attenuation of the electrons arriving at the wire, proportional to the drift distance. The amplitude of the electrons arriving at the wire is generally modelled as a decay function as following

$$Q_{Wire}(t) = Q_{Dep} \cdot \exp\left(\frac{-t}{\tau}\right) \tag{3.5}$$

where Q_{wire} is the charge collected on the wires at the anode plane, Q_{Dep} is the original deposited charge, t is the drift time and τ is the electron lifetime characterising the level of charge attenuation. A high electron lifetime, resulting from a low level of contamination is an extremely important operation parameter for a high efficiency energy reconstruction. Recently reported from ProtoDUNE, which utilised the same membrane cryostat technology as SBND, the experiment measured a lifetime of ≈ 10 ms, equivalent to an oxygen purity of 3.4 ppt []. This is much larger than the drift time of SBND (1.25 ms), making this effect almost negligible.

Space Charge Effect

An addition, argon ions produced as part of the ionisation process drift towards the cathode at a much slower velocity of 8×10^{-7} cm^2/s []. As SBND is a surface detector without an overburden, high exposure to cosmics rays results in a high rate of ionisation, and hence argon ions. The build up the argon ions causes a distortion in intensity and direction of the electric field, modifying the electron drift trajectory. This consequently impacts the charge deposition both spatially and calorimetrically. This effect is referred as Space Charge Effect (SCE) []. The calorimetry effect is due to the dependence of the recombination factor on the local distortion of the electric field. The spatial effect is due to the deformation of tracks drifting in distorted electric field, as shown in Fig. **??**. SCE leads to tracks appearing bowed and bent away from the detector edges.

Therefore, SCE worsens the spatial as well as energy resolution of a track reconstruction and consequently, particle identification. SBND will implement a dedicated laser calibration system [], as well as calibration using cosmics track crossing cathode and anode [] to model the distorted electric field. Once measured, correction will be applied in the reconstruction.

3.3.2 Photons Propagation

Rayleigh Scattering

Liquid argon is transparent its own scintillation light, and hence, the emitted photons are able to propagate over a long distance. Scintillation photons undergo different physical process as they propagate: Rayleigh scattering, reflections and refractions in the detector

material boundaries, and absorption due to contaminants. Rayleigh scattering is a first order effect, where photons elastically scatter off a nuclei, modifying their trajectories. Reflection off solid surfaces in the detector volume is a second order effect. Both of these effects do not change the number of photons, however alters the propagation paths of the photons. Particularly, this can lengthen the prompt component of scintillation photons, which is the main component for triggering (See Chapter **??**) and high timing precision analysis (See Chapter **??**). This effect can be either beneficial or detrimental to the probability of light arriving at the PDS, mainly depending on the position at the point of creation and the path taken. Consequently, this leads to a non-trivial distribution of photon arrival times at the PDS, ranging from a few to several tens of nanoseconds for a[]. The Rayleigh scattering length λ_{RS} in liquid argon has been reported from around 50 cm [] up to 110 cm [], which is comparable to the size of SBND.

Absorption

Furthermore, scintillation photons are can be absorbed by contaminants with a high cross section with VUV photons such as nitrogen [], methane []. Other elements such as ?? have also been observed in commercial argon []. The total absorption can be modelled as an exponential suppression of the number of photons as a function of the travelled distance, with absorption length as a parameter. The absorption rate is dependent on the Rayleigh scattering length, suchthat photons with shorter λ_{RS} undergoes longer and more indirect paths, increasing their probability of absorption before reaching the PDS.

Wavelength Shifting

Scintillation photons in the VUV range are typically absorbed by detector materials without being detected. An enhancement method for scintillation light signals in LArTPC is wavelength shifting. Specifically at SBND, TetraPhenyl Butadiene (TPB) is employed to shift the 128 nm wavelength photon to 430 nm, which is the visible light range. TPB is employed at two locations: TPB is evaporated onto the highly reflective Enhanced Specular Reflector (ESR) foils located at the cathode and TPC is coated on the optical windows of optical detectors. In the former method, VUV photons arriving at the reflective foils are wavelength-shifted and then reflected back towards the PDS located behind the cathode. In the latter method, VUV photons arriving at optical detectors are wavelength-shifted into detectable range of the detectors (See Chapter **??**).

The photon propagation is different for VUV versus visible range photons. As shown in Fig. **??**, due to high refractive index of liquid argon at VUV wavelenghts of ?? [], the group velocity of VUV photons is about twice slower than visible wavelengths photons. The Rayleigh scattering length for for VUV photons is two orders of magnitude smaller compared to visible photons, and thus VUV photons are less exposed to Rayleigh scattering and absorption probability.

This results in different arrival time and detection probability distributions, and consequently light yield for direct VUV light and reflected visible light as shown in Fig. **??**. Closer to the anode, the light yield primarily is from the direct light whereas closer to the anode, an hence the reflective foils, the light yield is from the reflected visible light. The combined light yield from both components result in an improved light yield and uniform distribution across the drift length of the detector. However, since the reflected light has to undergo a longer propagation paths, Rayleigh scattering and propagating towards the cathode, wavelength-shifting and reflecting back the full width of the detector before reaching the optical detector, the reflected light spatial distribution is more diffused and spread across a larger of optical detectors compared to direct light.

3.4 Detection of Charge and Light

3.4.1 Wire Readouts

Once arrive at the anode, the ionisation electrons induce signals on the readouts, which are typically made of three wire planes separated by a few mm. A bias voltage is applied to individual wire plane, allowing for electron transparency across the three planes. As shown in Fig. **??**, the drifted electrons induces bipolar signals on the two innermost planes and they pass through them, and hence, these planes are often referred to as the induction planes. The electrons are collected on the outermost plane, producing a unipolar signal. This plane is commonly known as the collection plane. The three planes are oriented 60° apart, minimising the impact of a track travelling parallel to a wire plane. Three dimensional spatial reconstruction of a track requires minimum at least two wire planes, however, many modern LArTPC experiments use all three planes [].

The signals induced or collected on the wire planes are then shaped, amplified and digitised by cold electronics before acquiring (See details in Chap. **??**). The amount of charge is correlated with the amount of energy deposited in the detector, accounting for additional corrections for the electron propagations effects (diffusion, attenuation, SCE, etc.) and

recombination effects. Finally, this allows for calorimetry and hence, particle identification to be performed.

3.4.2 Photomultiplier Tubes and X-ARAPUCA

Scintillation photons are detected by optical detectors located behind the wire planes. The primary detection technology is Photomultiplier Tubes (PMTs), with a Quantum Efficiency (QE) up to 30% []. However, PMTs are typically large and require a sufficient volume inside the detector for installation. Current and future experiments are increasingly shifting towards using Silicon Photomultipliers (SiPMs), due to their advantageous smaller size, lower power consumption, excellent signal to noise ratio and a high QE up to 40% []. X-ARAPUCA device is a novel light collection technology using SiPMs, currently being developed by Unicamp [] and tested inside the SBND detector. As shown in Fig. **??**, it is a light guide designed to trap light by a combination of wavelength shifter and dichroic filters. The dichroic filter is transparent to a narrow range of wavelengths and reflective otherwise, and thus, only photons of certain wavelengths can pass through the filter and cannot escape. The photons are internally reflected in the trap until detector by the SiPMs.

As discussed in Sec. **??**, both PMTs and X-ARAPUCAs are coated with TPB for wavelength shifting from 128 nm VUV scintillation photons to visible range, which is more easily observable for the optical detectors discussed here. The direction of re-emitted light is isotropic and hence, coated PDS suffers a 50% reduction in efficiency due to photons emitting away from the detection surface. TPB can also impact the detection time since the emission of visible photon is not instantaneous.Multiple time components of re-emission photons from TPB have been observed, of which the majority of photons are re-emitted within nanoseconds with a subset being re-emitted as long as a few microseconds [].

Finally, the waveforms of the photons are digitised and acquired using very high sampling frequency readout, ranging between 1-2 ns []. This makes scintillation light signal having much timing resolution compared to the charge signal, thus providing the most precise interaction timing information available in the detector, particularly useful for triggering and Heavy Neutral Lepton analysis (See Chapter **??**).

3.5 Concluding Remarks

References

[1] P. A. Machado et al., "The short-baseline neutrino program at fermilab", Annual Review of Nuclear and Particle Science **69**, 363–387 (2019).

[2] B. Abi et al. (DUNE), "Deep Underground Neutrino Experiment (DUNE), Far Detector Technical Design Report, Volume II: DUNE Physics", (2020).

[3] R. S. Jones, "Muon-neutrino disappearance with multiple liquid argon time projection chambers in the Fermilab Booster neutrino beam", PhD thesis (The University of Liverpool, 2021).